Neurocomputing 173 (2016) 1203–1210

Contents lists available at ScienceDirect

Neurocomputing

journal homepage: www.elsevier.com/locate/neucom

Wavelet decomposition and phase encoding of temporal signals using spiking neurons

Zhenzhong Wang, Lilin Guo, Malek Adjouadi *

Center for Advanced Technology and Education, Florida International University, 10555 West Flagler Street, EC 2220, Miami, FL 33174, USA

ARTICLE INFO

Article history:
Received 10 December 2014
Received in revised form
10 June 2015
Accepted 28 August 2015
Communicated by W.L. Dunin-Barkowski
Available online 8 September 2015

Keywords:
Spiking neuron
Leaky Integrate-and-Fire neuron
Digital signal processing
Interictal spike detection
Wavelet decomposition
Phase encoding

ABSTRACT

Spike encoding is the initial yet crucial step for any application domain of Artificial Spiking Neural Networks (ASNN). However, current encoding methods are not suitable to process complex temporal signal. Motivated by the modulation relationship found between afferent synaptic currents in biological neurons, this study proposes a spike phase encoding method for ASNN, which could perform wavelet decomposition on the input signal, and encode the wavelet spectrum into synchronized output spike trains. The spike delays in each synchronizing period represent the spectrum amplitudes. The encoding method was tested in two implementation examples: (a) encoding of human voice records for speech recognition propose; and (b) encoding of multichannel electroencephalography (EEG) records with the aim to detect interictal spikes in patients with epilepsy. Empirical evaluations confirm that encoded spike trains constitute a good representation of the continuous wavelet transform of the original signal, with the ability to capture interesting features from the input signal.

1. Introduction

The most significant difference between Artificial Spiking Neural Networks (ASNN) and traditional neural networks is that information in ASNN is represented by spike trains which are a series of pulses with timings of interests. There are mainly two kinds of interpretations developed in signal processing applications about how information is related to spike trains: (1) the rate encoding, which assumes that the information is encoded by the counts of spikes in a short time window; and (2) the spike time encoding which considers information carried at the exact time of each pulse in the spike train. Although the mechanisms for data representation and analysis using biologically-inspired neural networks is still under development, empirical evidence has shown that spike time encoding might be more reliable in explaining experiments on the biology of nervous systems [1,2].

Both rate encoding and spike time encoding essential in ASNN applications. The easiest way to rate encode an analog signal is to feed it to a Poisson neuron, which fires output spikes at probability proportional to its membrane potential, thus making its firing rate within a short time window proportional to the amplitude of the input signal. Such an encoding method has been adopted by Sprekeler et al. [3] and Keer et al. [4] in order to analyze the recurrent ASNN behaviors. Although Poisson neuron model is simple and suitable for theoretical analysis, it was rarely implemented in real-world applications due to its inaccuracy in mapping analog signals to spike trains. De Garis et al. [5] introduced another rate encoding method which deconvolves the input signal into its individual spike responses, so that the post-synaptic potential of the encoded spike train could be quite similar to the original signal. Schrauwen and Van Campenhout [6] improved algorithm proposed by De Garis et al. by optimizing the deconvolution threshold yielding the so-called Bens Spiker Algorithm (BSA). BSA has been used widely as a rate encoding method for ASNN applications [7–9]. The major problem of this type of rate encoding is that an averaging time window is required for each sampling of the input signal, which as a consequence limits the temporal resolution of the encoded signals.

In order to overcome this drawback, receptive fields are introduced by other researchers to improve the temporal resolution [10,11], where input signals are first decomposed by Gaussian windows with variant shifts of the window center, and then fed to an array of neurons which convert them to multiple spike trains. Address-Event Representation (AER) is an asynchronous protocol designed for analog neural system simulation platforms [12]. However, AER is also referred to as an encoding method by other groups of researchers [13–15]. When used as an encoding method, encounters of “ON” and “OFF” events in the input signals are registered by AER to generate corresponding output spikes. The “ON” and “OFF” events in AER indicate the time when a change in the input signal either exceeds a positive threshold or fall behind a negative threshold. Under such definition, AER could be treated as a rate encoding method with regards to the derivatives of the input signal.

* Corresponding author. Tel.: +1 305 348 4106.
E-mail address: adjouadi@fiu.edu (M. Adjouadi).

http://dx.doi.org/10.1016/j.neucom.2015.08.078
0925-2312/

Synchronized spike time encoding, dubbed as Phase Encoding (PE), was also widely used in ASNN application. A simple implementation of PE could be realized by linearly mapping the input signal to the delay of spikes within each synchronizing period [16]. This implementation of PE requires the input signal either to be static or vary at frequencies much lower than the synchronizing frequency. Temporal receptive fields could also be utilized for PE to improve the encoding resolution [17,18]. To be more biologically plausible, Rumbell et al. [19] introduced a synchronizing method which considered spiking neurons as PE units instead of performing linear mapping between analog values and spike delays. Receptive fields in this study were applied to the amplitude dimension instead of the temporal dimension, which yielded good performance for static input data. However, PE method which could accurately encode temporal signals is still under development.

Beside receptive fields, wavelet transform is another useful approach to pre-process input signals before encoding them into spike trains. Wavelet transform is commonly used as a preprocessing method for using ASNN for image classification [20,21] or computer vision tasks [22,23]. The generated wavelet coefficients are in general much less variable than the raw signals, which makes it easier for rating or phase encoding the coefficients into spike trains. However, current encoding schemes for ASNN which incorporates wavelet transform all apply wavelet decompositions off-line, and operates outside the ASNN platform, which makes the encoding scheme inefficient for encoding prolonged temporal signals.

In this paper, we propose a preprocessing unit for the Leaky Integrate-and-Fire (LIF) spiking neurons. The assumption is that an encoding device combining the preprocessing unit with a LIF neuron could be used to encode analog signals with wide frequency range. We will demonstrate in Section 2 that our preprocessing unit could decompose the input signal into wavelet spectrum, and further encode the spectrum amplitude into the delay amount between output spikes and the clock signals. Empirical results of PE encoding of two different types of signals (speech and EEG signals) are provided in Section 2.5, with linearity, temporal resolution issues and possible extension of the encoding method discussed.

2. Methods

In this section, we will demonstrate that an array of specially designed encoding devices could perform wavelet decomposition of temporal signals. We purposely designed the encoding device by incorporating a two-stage spike triggered modulate-and-integrate module with traditional LIF neurons, and made such pre-processing module compatible with ASNN platform, so that the encoding device is easy to implement on any ASNN platforms. Inspired by the multiplication relationship found among afferent synaptic currents in biological neurons [24], we found that delay synchronized spikes sent to the two synapses integrated in the special designed LIF neuron could trigger the wavelet transform of the input signal at certain time scales, and encode the spectrum amplitudes into delays between the output fire times and the control spike arriving times. Simulations in this research were conducted using NEural Simulation Tool [25] (NEST) with the encoding device implement and integrate into the simulation kernels.

2.1. LIF encoding

Spiking neuron models are typically a set of Ordinary Differential Equations (ODE) which attempt to capture the dynamics of the neuron membrane potential. Different neuron models have been proposed by researchers to mimic the electrical behaviors of biological neurons. Among these neuron models, LIF model was believed to be a reasonable simplification of biological neuron with balanced accuracy and efficiency. LIF spiking neuron is described by one-dimensional ODE using the following equations:

$$\tau\frac{du(t)}{dt} = -u(t)+\frac{\tau}{C_m}I_{all}(t) \tag{1}$$

where u is the membrane potential, τ and C_m are the time constant and capacitance of the neuron, respectively, with I_{all} defining the overall afferent current. The firing condition and post-fire behavior of the LIF neuron in (1) can be defined by the following equation:

$$\text{if } u = u_{th} \quad \text{and} \quad \frac{du(t)}{dt} > 0, \quad u \leftarrow u_c \tag{2}$$

where u_{th} is the firing threshold and u_c is the post-fire resetting potential. Note that a derivative condition is applied to the firing conditions in the same manner as in Wang et al. [26]. Such derivative condition ensures that the neuron only fires when its membrane potential in an upward trend crosses the threshold, a condition which is thus set to avoid accidental fires if the resting potential of the neuron is higher than its firing threshold.

The stimulation to LIF neuron is typically assumed to be a summation of all weighted synaptic currents and an external current:

$$I_{all}(t) = I_e(t)+\sum_j w_j I_s(t-s_j) \tag{3}$$

In this equation, $I_e(t)$ is the external current, $I_s(t)$ is the shape function of the post-synaptic current (PSC), s_j is the time that the j-th spike arrives at the synapse, and w_j is the connection efficacy corresponding to the j-th input spike.

Consider a quasi-static input signal being used as the external current to the LIF neuron, and no synaptic stimulation was connected, (1) could be solved as

$$u(t) = u_c\exp\left(-\frac{t-t^f}{\tau}\right)+\tau I_e(t)\left[1-\exp\left(-\frac{t-t^f}{\tau}\right)\right]/C_m \tag{4}$$

where t^f is the most recent fire time of the LIF neuron. The output spike interval T is thus a function of I_e as defined below

$$T = \tau\ln\left(\frac{u_c C_m-\tau I_e}{u_{th}C_m-\tau I_e}\right) \tag{5}$$

Since the reset potential is usually lower than the threshold u_{th}, larger I_e yields shorter spike interval and thus higher firing rate over a short time window. The input signal is rate encoded in this configuration.

Rumbell et al. [19] suggested a method to generate phase encoded spike train using LIF neurons. A global inhibitory neuron has been connected to all encoding neurons, so that the reset times of these neurons are synchronized, and the firing time interval found in (5) could be converted into the firing delays between neurons.

Encoding methods using LIF neurons however suffer from one major drawback in that the input signal should be quasi-static in comparison to the time constant of the LIF neuron. Although temporal decomposition methods such as Gaussian receptors could reduce the fluctuation of the input signal, the number of receptors increase dramatically with increasing frequency of the input signal, which prevents the encoding method from capturing fast transients in the input signals.

2.2. Spike triggered modulation

Although linear summation of synaptic currents and external current as performed in (3) has been widely accepted as a simplified relationship among the afferent stimulations in large scale ASNN, the interaction between post-synaptic currents was found to be more complicated in biological nervous system. Koch and Segev [24] found that biological neurons might approximate sum

of products among different groups of synaptic currents. Inspired by this finding, we designed an artificial wavelet decomposition and spike phase encoding device incorporating a two-stage modulate-and-integrate module, where the multiplication is performed instead of summation between the input signal and synaptic currents. The first stage of the module incorporates the integration of the multiplication of external current and a wavelet shape synaptic current, while the second stage modulate the output from first stage with an exponential decay synaptic current. We will prove that using our preprocessing module together with a LIF neuron, input signal could be decomposed into wavelet spectrum and such spectrum amplitude could be encoded into synchronized spike trains.

In reference to Fig. 1, C_{int} and C_{enc} are delay synchronized clock spikes satisfying:

$$t_i^{\text{enc}} - t_i^{\text{int}} = T_{\text{e}} \tag{6}$$

where T_{e} is the delay phase, t_i^{int} and t_i^{enc} are time of spikes in C_{int} and C_{enc} respectively, with $i = 1, 2, \ldots, n$ being the index of each spike. The interval of spikes in both C_{int} and C_{enc} is T_{clk}. C_{int} and C_{enc} are converted into post-synaptic current I_{enc} and I_{int} by synapse S_{int} and S_{enc} respectively. Input signal I_{e} is multiplied with I_{int}, and integrated by neuron N_{int} into its state variable v. N_{enc} is a normal LIF neuron, stimulated by the absolute amplitude of v modulated with I_{enc}.

The overall dynamics of this encoding unit could be specified by the following equations:

$$\tau \frac{du(t)}{dt} = -u(t) + \frac{\tau}{C_{\text{m}}} |v(t)| I_{\text{enc}}(t) \tag{7}$$

$$a \frac{dv(t)}{dt} = I_{\text{e}}(t) I_{\text{int}}(t) \tag{8}$$

where u is the state variable of N_{enc}, I_{enc} and I_{int} are summations of the post-synaptic currents of spikes in C_{enc}, and C_{int} respectively, and are defined as follows:

$$I_{\text{enc}}(t) = \sum_i \exp\left(-\frac{t - t_i^{\text{enc}}}{\tau}\right) \Theta(t - t_i^{\text{enc}}) \tag{9}$$

$$I_{\text{int}}(t) = \sum_i \sqrt{a} \Psi\left(t - t_i^{\text{int}} - d, \sigma\right) \Theta\left(t - t_i^{\text{int}}\right) \tag{10}$$

where Ψ is a wavelet mother function used as the PSC for S_{int}, with a representing the scale of the wavelet, $\sigma = af_s$ indicating the time scale of the wavelet related to the sampling frequency f_s, d serving as an offset parameter, and Θ being a Heaviside step function. We selected a shifted Mexican-hat wavelet mother function for Ψ as a demonstration here:

$$\Psi(t, \sigma) = \frac{2}{\sqrt{3}\pi^{1/4}} \left(1 - \frac{t^2}{\sigma^2}\right) \exp\left[-\frac{t^2}{2\sigma^2}\right] \tag{11}$$

Assuming that the length of integration period T_{i} satisfies $T_{\text{i}} < T_{\text{clk}}$, we could define $d = T_{\text{i}}/2$ in (10), so that the wavelet function is centered within each integration window. The concept of wavelet mother function will be discussed in Section 2.5. Note that both I_{enc} and I_{int} are constructed in a unitless manner for the model simplification.

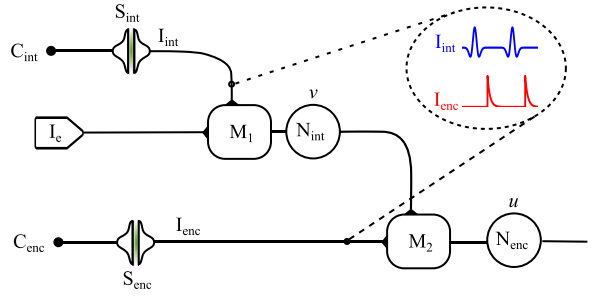

Fig. 1. Wavelet decomposition and spike phase encoding device with two-stage modulate-and-integrate module.

Suppose that each spike in C_{int} could reset the state variable v of neuron N_{int} to zero, and that σ is significantly smaller than T_{clk}, then (7) could be solved for $t_i^{\text{int}} \le t < t_{i+1}^{\text{int}}$ as

$$v(t) = \frac{1}{\sqrt{a}} \int_{t_i^{\text{int}}}^{t} I_{\text{e}}(\zeta) \Psi\left(\zeta - t_i^{\text{int}} - T_{\text{i}}/2, \sigma\right) d\zeta \tag{12}$$

Suppose further that σ is significantly smaller than T_{i} , and consider that $\Psi(t, \sigma) \to 0$ when $t > T_{\text{i}}$ or if $t < 0$, then (12) could be approximated by

$$v(t) = \frac{1}{\sqrt{a}} \int_{-\infty}^{\infty} I_{\text{e}}(\zeta) \Psi\left(\zeta - t_i^{\text{int}} - T_{\text{i}}/2, \sigma\right) d\zeta = X_{\text{w}}\left(t_i^{\text{int}} + T_{\text{i}}/2, \sigma\right) \tag{13}$$

for $t_i^{\text{int}} + T_{\text{i}} \le t < t_{i+1}^{\text{int}}$, where X_{w} is the wavelet transform of input I_{e} at translation $t_i^{\text{int}} + T_{\text{i}}/2$ and time scale σ.

Assuming that

$$T_{\text{i}} < T_{\text{e}} < T_{\text{clk}} \tag{14}$$

and suppose each input spike from C_{enc} could reset the state variable from u to u_c for neuron N_{enc}, (7) could be solved for $t_i^{\text{enc}} \le t < t_{i+1}^{\text{enc}}$ as

$$u(\Delta t) = u_{\text{c}} \exp(-\Delta t/\tau) + V(\Delta t) \tag{15}$$

$$V(\Delta t) = \frac{\tau \Delta t}{C_{\text{m}}} \exp(-\Delta t/\tau) \left| X_{\text{w}}\left(t_i^{\text{int}} + T_{\text{i}}/2, \sigma\right) \right| \tag{16}$$

where Δt is the elapsed time since last input spike from C_{enc} arrives at the neuron. Note that the absolute value operation applied to v makes $V(\Delta t)$ a function of the absolute spectrum of the wavelet transform X_{w}. The absolute spectrum is preferable to power spectrum of wavelet transform, in the sense that it ensures that the units in (15) are balanced without need for extra constants.

We considered two different combinations of reset potential u_{c} and output firing threshold u_{th} for N_{enc}:

(i) Negative threshold: $u_{\text{c}} < u_{\text{th}} < 0$.
(ii) Positive threshold: $u_{\text{c}} = 0$ and $u_{\text{th}} > 0$.

In the first combination, as long as

$$T_{\text{clk}} - T_{\text{e}} > \tau \ln\left(u_{\text{th}}/u_{\text{c}}\right) \tag{17}$$

$V(\Delta t)$ is a non-negative function. The membrane potential will exceed the threshold and an output spike will be generated during each time segment $[t_i^{\text{enc}}, t_{i+1}^{\text{enc}})$. The fire delay T in the i-th segment could be solved from

$$|X_{\text{w}}| = \frac{C_{\text{m}}}{\tau T} \left[u_{\text{th}} \exp(T/\tau) - u_{\text{c}}\right] \tag{18}$$

where T is guaranteed to be a monotonic decreasing function of $|X_{\text{w}}|$.

For the second combination, consider that $V(\Delta t)$ is a bell shape function which reaches its maximum when $\Delta t = \tau$, the membrane potential could exceed the threshold only if the wavelet spectrum amplitude satisfies

$$|X_{\text{w}}| \ge X_{\text{th}} = \frac{u_{\text{th}} C_{\text{m}}}{e\tau^2} \tag{19}$$

in which case the firing delay T could be solved from

$$|X_{\text{w}}| = \frac{u_{\text{th}} C_{\text{m}}}{\tau T \exp(-T/\tau)} \tag{20}$$

Note that T is always less than τ in (20), which ensures that T is a monotonic decreasing function of $|X_{\text{w}}|$ when the amplitude

spectrum $|X_w|$ is larger than the threshold X_{th}. If the wavelet spectrum amplitude is smaller than X_{th}, the LIF neuron N_{enc} will not fire during $[t_i^{enc}, t_{i+1}^{enc})$.

In both combinations discussed above, the wavelet spectrum of input signal I_e is encoded into delay phase T which is the difference between the time of each output fire and the arrival time of the most recent input spike in C_{enc}. Thus, larger wavelet spectrum amplitude corresponds to faster firing after each clock spike.

2.3. Wavelet encoding device implementation

Synapses and neurons as described in (7) through (11) are implemented in NEST with a single customized numeric model referred to as the Wavelet Encoding Device (WED). In order to balance the accuracy and efficiency while solving ODEs for WED, exponential integration method has been adopted to solve the state variable u, and Simpson's rule was applied to the integration for state variable v:

$$u_{n+1} = P_{32} s_n |v_n| + P_{33} u_n \tag{21}$$

$$v_{n+1} = \frac{h}{6}\left(I_m(t_n) + 4I_m\left(t_n + \frac{h}{2}\right) + I_m(t_n + h)\right) + v_n \tag{22}$$

$$s_{n+1} = P_{33} s_n \tag{23}$$

$$I_m(t) = P_2\left(1 - \frac{\delta t^2}{\sigma^2}\right)\exp\left(-\frac{\delta t^2}{2\sigma^2}\right) I_e(t) \tag{24}$$

$$\delta t = t - T_i/2 - t^{int} \tag{25}$$

where subscript n indicates the n-th simulation step, h is the simulation step size, t^{int} is the arrival time of the most recent spike in C_{int}, and P_2, P_{32} and P_{33} are constant parameters defined by the following relations:

$$\begin{aligned} P_2 &= \frac{2}{\sqrt{3a}\pi^{1/4}} \\ P_{32} &= \frac{\sigma\tau}{C_m}\left[1 - \exp(-h/\tau)\right] \\ P_{33} &= \exp(-h/\tau) \end{aligned} \tag{26}$$

Each WED incorporates two types of spike receptors to distinguish whether a spike is send to S_{int} or S_{enc}, in the same manner as any other neuron model implemented in NEST which could receive spike input from more than one type of synapses. Input spikes with receptor type I are recognized as spikes sent to S_{int}, which could reset v_n to zero and set t^{int} to the current time; while input spikes with receptor type II are recognized as spikes sent to S_{enc}, which in turn could reset u to u_c and s to zero.

A normal LIF neuron N_{clk} with an exponential decay synapse is implemented in this network as the clock generator. This LIF neuron is connected to itself with axon delay T_{clk} and synaptic efficacy large enough to generate a new output spike from itself. A short strong pulse injected to N_{clk} could initialize the first firing of N_{clk}, and generate oscillatory clock spikes at constant interval approximate to T_{clk}. These clock spikes are sent to type I receptors in WED with a short delay D_0, and type II receptors with a longer delay T_e.

The structure of the encoding network depends on the type of application. Two different structures were implemented in our research to encode two types of signals: human voice records and multi-channel EEG signals.

2.4. Encoding human voice record

An encoding network was implemented to convert the human voice records obtained from Census Database of Carnegie Mellon University [27] (AN4) into spike trains related to the wavelet spectrum. An array of 100 WEDs with parameters $\tau = 45$ ms and σ varies between 0.2 ms and 10.0 ms were implemented in the encoding network. The spike trains could encode frequency components ranging from 100 Hz to 50 kHz in the input signal, which is wider than the human voice frequency limitations. Time constants $T_{clk} = 100$ ms, $D_0 = 1.0$ ms, $T_i = 45$ ms, and $T_e = 50$ ms were selected to meet all the requirements posed by (14). A negative threshold $V_{th} = 1.0$ mV was used in this implementation. The reset membrane voltage was set to $u_c = 2.72$ mV so that the longest spike delay is $T_{max} = 45$ ms, according to the solution of (15) with $V(T) = 0$ mV and $u(T_{max}) = u_{th}$. Since $T_e + T_{max} < T_{clk}$, there is always one output spike from each WED within one clock cycle.

2.5. Encoding multi-channel EEG signal

Scalp EEG recordings from a patient with focal epileptic seizures was used as input signal in this application. The EEG recordings consist of 19 individual channels, each sampled at 512 Hz frequency. We implemented 19 groups of WED arrays, each connected to one individual channel of the EEG signal. Time constants $T_{clk} = 200$ ms, $D_0 = 1.0$ ms, $T_i = 85$ ms, $T_e = 100$ ms and $\tau = 100$ ms were used for all WEDs in this network.

The features of interests in the EEG recordings are the interictal spikes (IS) as described in [28], which in epilepsy are a key feature used for 3D source localization of seizure onsets. The detection of IS will also help delineate EEG records that could lead to seizures [29]. IS could be found in synchrony in multiple channels between ictal events, characterized as fast EEG transients (faster than 50 ms) with steep rising and falling slopes, and habitually followed by a slow potential. Since the shape of IS is similar to the Mexican-hat wavelet mother function, WED with time scale matched to the duration of these spikes will generate much faster output spikes. We built 50 WEDs for each EEG channel, with σ varies between 5 ms and 70 ms. A positive threshold $u_{th} = 0.5$ mV was implemented in this network, which ensures that WEDs only generate output spike when an IS is detected, and remain quiet otherwise. All channels of EEG recordings are pre-processed by a fifth-order Butterworth high-pass filter to avoid the influence of stochastic drifts. A 5 Hz cut-off frequency was used for this high-pass filter, so that high frequency features, especially the IS peaks are well preserved after the pre-processing.

3. Results

The record file “an253-fash-b.raw” from the training set of AN4 database was used as the input to the WED network. The state variables of each WED were recorded for the testing purpose. A portion of the recorded variables of one WED with $\sigma = 5.64$ ms was captured and plotted in Fig. 2.

Vertical red dash lines in Fig. 2 represent the arrival times of the clock spikes for the type I synapse receptor of this neuron. Input I_e was modulated with the wavelet kernel for 45 ms after each clock signal. When I_e contains components matching the 5.64 ms time scale of the wavelet function, the WED generates a larger modulated current, yielding as a consequence a larger state variable v. The clock spikes arrive at the type II synapse receptor of this WED after 50 ms delay (indicated by the green vertical lines in Fig. 2), which trigger the encoding periods. At the beginning of each encoding period, the integration of v has already finished, thus v holds its value for the whole encoding period. The LIF neuron incorporated by the WED would encode the constant v into an output firing delay. It could be found from the records of u that, WED generate output spikes faster when the input signal I_e contains components matching $\sigma = 5.64$ ms (i.e., periods from 3520 ms to 3720 ms), yet fires slower at almost the end of each encoding period when I_e contains only higher frequency components (i.e., periods from 3120 ms to 3320 ms).

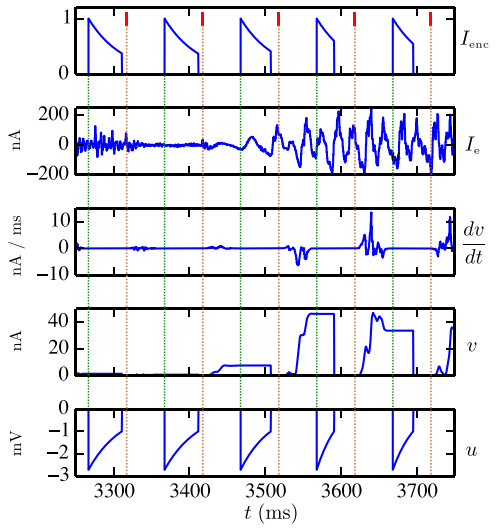

Fig. 2. Time course of variables in one WED with $\sigma = 5.64$ ms. Red vertical dash lines indicates the arrival times of spikes in C_{int}; green dash lines indicates the arrival times of spikes in C_{enc}. (For interpretation of the references to color in this figure caption, the reader is referred to the web version of this paper.)

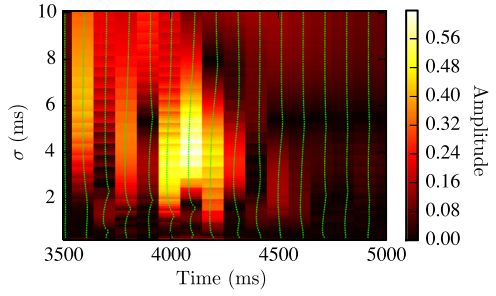

Fig. 3. Comparison of WED encoding with Continuous Wavelet Transform at corresponding translations. Green lines bars output spikes from the WED array. (For interpretation of the references to color in this figure caption, the reader is referred to the web version of this paper.)

The voice record used in this experiment was the sound of female pronouncing the word “GO”. The output spikes of all 100 WEDs were raster-plotted for the time range from 3500 ms to 5000 ms using short vertical green bars as shown in Fig. 3. Continuous wavelet transform using Mexican-hat wavelet was also applied to the same voice record. The wavelet transform at translations $t_i^{clk} + 22.5$ ms were color coded and superimposed on Fig. 3, where t_i^{clk} are the firing times of N_{clk}. It could be found from Fig. 3 that, the change of the fundamental frequency when pronouncing the word “GO” was clearly captured by the Mexican-hat wavelet transform, and the delay phases of WED output spikes were a good representation of the wavelet spectrum amplitudes during each clock cycle. Such phase encoded spike trains are applicable to any supervised spiking neural learning methods such as ReSuMe method [30], Multi-spiking neural network [31], Synaptic Weight Association Training [32], Spike Pattern Association Neuron [33], or online learning with adaptive structure [26]; or any unsupervised learning methods such as Rank Order Learning [14] or Spiking Self-Organizing Map [19,34]. Thus, the clustered or classified features of the frequency changes could be used to recognize the word pronounced. The phase delays of the WED array in this example could substitute for the spectrogram in estimating key characteristics in speech recognition [35], and could support the building of speech perception system using ASNN.

A portion of multi-channel EEG recordings with IS identified was plotted in Fig. 4, as well as the WED encoding results. Note that the

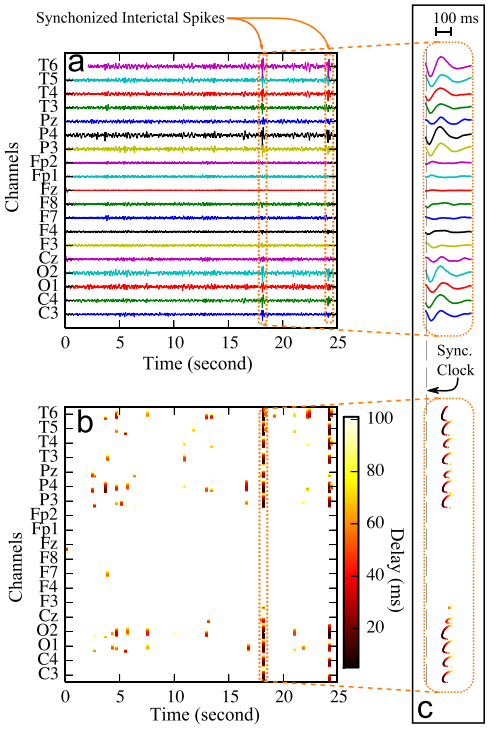

Fig. 4. Encoding of interictal spikes in a segment of multi-channel EEG recordings: (a) the waterfall plot of the recorded EEG potentials; (b) the pseudo color mapping of the encoded output spike delays; (c) detailed view of the IS wave found at approximately 18th second in the upper portion, and output spikes generated by WEDs in the lower portion.

delays of output spikes are color coded for each clock cycle and those clock cycles with no output spike were filled with “NAN” values and plotted as white blocks. We could find from Fig. 4(a) that there are two occurrences of synchronized IS in this segment of EEG recording. The zoomed view of the first IS at 100 ms scale as illustrated in Fig. 4(c) show that identified interictal spikes meet the criteria that characterize them, including sharp rising and falling edges, larger peak amplitudes and synchronization in multiple channels. These two IS strikes were accurately captured by the WED network. In Fig. 4(c), it was determined that only the WED groups which were connected to the EEG channels with IS presented fired output spikes, and the WED with wavelet time scale best matches the IS width fires faster than other WEDs in the same group. Although there were false positive WED output spikes generated at occasions when no IS was identified, the temporal and spatial sparseness of these output spikes make it possible to filter out such false positives using any spiking learning methods.

4. Discussion

As discussed in the previous section, the encoding results from WED network are identical to regular wavelet decomposition results, which proves that WED is a reliable wavelet decomposing and spike phase encoding method for input signals on ASNN platform. Compared to applying regular wavelet decomposition to input signals before feeding them to ASNN, WED network has the following advantages:

(a) WED is ASNN platform compatible. Moreover, WED is designed by combining an ASNN platform compatible preprocessing module and a regular LIF neuron, making it easier to implement and integrate to an ASNN platform; while integration of a regular wavelet transform algorithm to ASNN

platform is typically much harder, even impossible for analog ASNN platforms.

(b) WED could encode input signals online, while previous wavelet decomposition pre-processing methods are mostly off-line. Without WED, complex synchronizing mechanism is required among wavelet transform device, phase encoding device and ASNN platform for an ASNN application to perform wavelet decomposition pre-processing on-line. Yet WED is automatically synchronized with ASNN platform, benefiting from the spike triggered module design.

(c) WED is more efficient. Theoretically, the wavelet transform only performs on certain translations when trigger spikes arrive, thus avoiding unnecessary calculations in regular wavelet transform algorithm. The possibility of implementing WED on analog ASNN platform could further enhance the parallel computing power of WED.

Some other features found unique in WED method are discussed in this section to further reveal the encoding properties of WED network.

4.1. Encoding non-linearity

The logarithm relationship between stimulation intensity and the delay phase of encoded spikes in sensory neurons was identified by many neurologists [36]. In many spiking neural network applications which implements PE as the sensing method, a log function was applied to the input signals to mimic the logarithm relationship [9,18]. Encoding using WED is highly nonlinear according to (18) and (20), yet the logarithmic relationship between stimulation intensity and the delay phase of spikes is a natural feature of WED.

As shown in Fig. 5, the linearity between $\log(|X_w|)$ and $\log(T)$ could be found in certain regions for the five selected WEDs with time constants τ being 20 ms, 40 ms, 60 ms, 80 ms and 100 ms, respectively. In Fig. 5(a), positive firing threshold was adopted for these neurons, and the wavelet spectrum amplitude threshold was set to $X_{th}=10^{-3}$ for all five neurons. The firing threshold u_{th} for these neurons could be calculated by (19). We could find that WED could encode $\log(|X_w|)$ to $\log(T)$ in a linear way when $|X_w|$ is in the linear region shown in Fig. 5(a). Different time constants τ introduce different offsets to the linear relationship along the y-axis: larger τ values corresponds to better encoding resolution for small $|X_w|$.

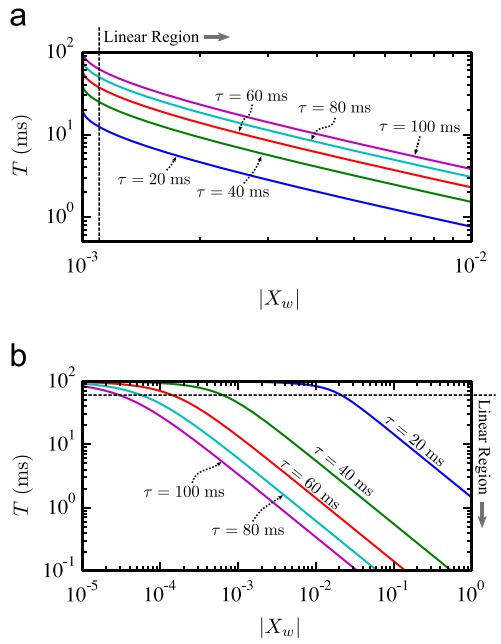

Fig. 5. Logarithm relationship of the input intensity and output spike delay: (a) the relationship of positive threshold WEDs; (b) the relationship of negative threshold WEDs.

As a comparison, negative firing threshold were used for the WED in Fig. 5(b), with u_{th} all set to -0.2 mV. u_c for these neurons was adjusted according to

$$u_c = u_{th}\exp(\tau_{max}/\tau) \tag{27}$$

such that the maximum output fire delay was always $T_{max}=100$ ms. Linearity could also be found in the linear region indicated in Fig. 5(b), when T is a bit smaller than T_{max}. Different time constants τ introduce different offsets to the linear relationship along the x-axis.

It should be noted that, using the same τ settings, negative firing thresholds provide better logarithm linearity than positive firing thresholds for the encoding of signals with a larger range of $|X_w|$. Since the parameter τ in WED is limited by the encoding window length, negative firing thresholds could be a better choice when the encoding linearity is of interest, as demonstrated in this paper when encoding was performed on the example of the human voice record. However, the $|X_w|$ cut-off feature provided by the positive firing thresholds could be useful when only large values of $|X_w|$ are of interest, such as in the case of IS detection for EEG recordings. The threshold configuration as well as the time constant τ should thus be carefully selected for a given application, so that the features of interest in the input signal could be best encoded into the delay of output fires.

4.2. Mother wavelet functions

Although a shifted Mexican-hat wavelet mother function was used for the post-synaptic current shape function in S_{int}, it is not required for WED to work properly. Any types of wavelet mother functions could be used as the current shape function in WED, and the input signal will be decomposed according to the mother wavelet functions selected. If a discrete wavelet is demanded, the kernel function of the discrete wavelet at different time scale with proper shifting should be used as Ψ in (10).

More interestingly, since the integration of the wavelet kernel performs only in a limited time duration, the only requirement for $\Psi(t)$ is that

$$\lim_{t\to\pm\infty}\Psi(t)=0 \tag{28}$$

and $\Psi(t)$ is not required to be absolutely integrable and square integrable from $-\infty$ to $+\infty$. Some functions, such as the alpha function

$$\Psi_\alpha(t,\sigma)=\frac{t}{\sigma}\exp\left(-\frac{t}{\sigma}\right) \tag{29}$$

could also be used to decompose the input signals.

The results shown in Fig. 6 illustrate the encoding of Human Voice Record using Mexican-hat function and Alpha function as the decomposing kernels. The phase encoding using WEDs with Mexican-hat kernel yields similar results compared to those using Alpha function kernel, except the time scales of Mexican-hat kernel are related to those of Alpha functions with the following constant ratio:

$$\frac{\sigma_m}{\sigma_\alpha}=2.784 \tag{30}$$

This is a reasonable representation of the differences between the central frequencies of the Mexican-hat kernel and the Alpha function kernel. Functions, such as Alpha function illustrated above, are more biological plausible, thus more likely to be implemented on an analog ASNN simulation platform.

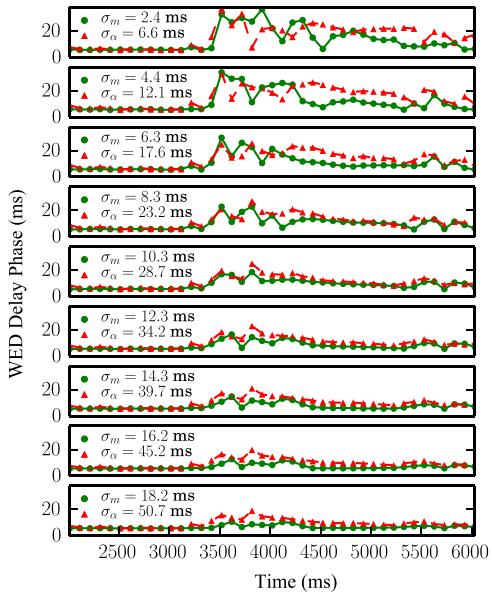

Fig. 6. Comparison between WED encoding using Mexican-hat wavelet and Alpha function. The σ_m are the time scales used for WED with Mexican-hat wavelet kernels while σ_α are the corresponding time scales used for WED with Alpha function kernels.

4.3. Temporal resolution

Since the wavelet of a WED is convolved with the input signal only once during each clock cycle, the encoding temporal resolution of one WED is limited to the clock interval T_{clk}. Considering that the total of integration time T_i and that encoding time T_e should be smaller than T_{clk}, and the time constant τ should also be smaller than T_i, although a decreased T_{clk} could enhance the encoding temporal resolution, it might also harm the encoding range of the wavelet spectrum amplitude. In order to enhance the temporal resolution of a WED array without interfering with the encoding range, we could still implement multiple WEDs for each time scale selection, but with different D_0 values. Accordingly, the wavelet transform would be performed at different translations within each clock cycle, and thus could significantly enhance the temporal resolution of the encoding without shrinking the length of each clock cycle.

5. Conclusion and future work

Encoding of analog signals into spike trains is one of the most important steps for information processing in biological nervous systems. The encoding method we proposed in this paper incorporates the concepts of synaptic current modulation with phase encoding representation. We proved that the proposed wavelet encoding device combining a preprocessing unit and a LIF neuron could perform the wavelet decomposition of the input signal, and convert the wavelet spectrum amplitude at certain translation and time scales into delays of output spikes.

Encoding networks using WED were implemented in this study to encode an example of a human voice record, with results that are quite similar to continuous wavelet decomposition. The encoding method was also applied to multi-channel EEG records of epilepsy patients to detect the IS to guide the prognosis of epilepsy and to determine the 3D source localization of the epileptogenic zone. We found that when WEDs contains wavelet kernel with time scales matched to the expected durations of IS, they could detect these IS events, and accurately preserve the synchronizing behavior of IS in the output spike trains for enhanced diagnosis and 3D source localization. The linearity property and limitations of mother wavelet functions of this encoding method were discussed as a guidance for choosing proper parameters for the WED network to fit a specific application. We also provide a simple method to overcome the temporal resolution limitation posed by the clock signal, so that the wavelet decomposition could be performed with higher temporal accuracy if needed.

Beyond the above contributions, this work also provides an intuitive insight of how stimulations gathered by sensor neurons might be represented and processed by a biological nervous system: the modulation behavior found between dendrites together with the integration feature of a biological neuron could perform decomposition of stimulation signals similar to wavelet transforms, and encode only those features of interest in the stimulation into the spike delay phases.

There are other possibilities for using the proposed encoding method such as: (1) apply graph theory [37] to find the connectivity between encoded spike trains, or (2) build spiking self organizing map and supervised learning systems to further process the encoded spike trains, and classify the patterns represented by the encoded spike trains into meaningful symbols. Since wavelet decomposition is also an important tool in feature extraction step for EEG signal processing [38], WED could facilitate EEG processing with a new online and biological plausible way to extract features from the EEG channels. EEG classification tasks based on certain frequency bands [39,40] could also benefit from the multidimensional transform inherited in WED. Although WED and the encoding network were implemented in the NEST environment, which is based on a digital computing platform, the design concepts are fully compatible with analog computing. We are interested in developing analog circuits to implement an encoding network, so that Ultra Large Scale Integration methods could be used to build a highly parallel neuromorphic system.

Acknowledgments

The authors are extremely grateful for the support provided by the National Science Foundation under Grants CNS-0959985, CNS-1042341, HRD-0833093, IIP-1338922, and CNS-1429345. The generous support of the Ware Foundation is also greatly appreciated.

References

[1] S. Panzeri, R.S. Petersen, S.R. Schultz, M. Lebedev, M.E. Diamond, The role of spike timing in the coding of stimulus location in rat somatosensory cortex, Neuron 29 (3) (2001) 769–777.
[2] R.S. Johansson, I. Birznieks, First spikes in ensembles of human tactile afferents code complex spatial fingertip events, Nat. Neurosci. 7 (2) (2004) 170–177.
[3] H. Sprekeler, C. Michaelis, L. Wiskott, Slowness: an objective for spike-timing-dependent plasticity?, PLoS Comput. Biol. 3 (6) (2007) 1136–1148.
[4] R.R. Keer, A.N. Burkitt, D.A. Thomas, M. Gilson, D.B. Grayden, Delay selection by spike-timing-dependent plasticity in recurrent networks of spiking neurons receiving oscillatory inputs, PLoS Comput. Biol. 9 (2) (2013) e1002897.
[5] H.D. Garis, M. Korkin, F. Gers, E. Nawa, M. Hough, Building an artificial brain using an FPGA based CAM-Brain Machine, Appl. Math. Comput. 111 (2–3) (2000) 163–192.
[6] B. Schrauwen, J. van Campenhout, BSA, a fast and accurate spike train encoding scheme, in: International Joint Conference on Neural Networks, vol. 4, 2003, pp. 2825–2830.
[7] N. Nuntalid, K. Dhoble, N. Kasabov, EEG classification with BSA spike encoding algorithm and evolving probabilistic spiking neural network, in: B.-L. Lu, L. Zhang, J. Kwok (Eds.), ICONIP, vol. 7062, Springer, Berlin, Heidelberg, Shanghai, China, 2011, pp. 451–460.
[8] Y. Chen, J. Hu, N.K. Kasabov, Z. Hou, L. Cheng, NeuCubeRehab: a pilot study for EEG classification in rehabilitation practice based on Spiking Neural Networks, in: M. Lee, A. Hirose, Z.-G. Hou, R. Kil (Eds.), ICONIP, Springer, Berlin, Heidelberg, Daegu, Korea, 2013, pp. 70–77.
[9] N. Kasabov, K. Dhoble, N. Nuntalid, G. Indiveri, Dynamic evolving spiking neural networks for on-line spatio- and spectro-temporal pattern recognition, Neural Netw. 41 (2013) 188–201.

[10] N.R. Luque, J.A. Garrido, J. Ralli, J.J. Laredo, E. Ros, From sensors to spikes: evolving receptive fields to enhance sensorimotor information in a Robot-Arm, Int. J. Neural Syst. 22 (4) (2012) 1250013.
[11] S. Schliebs, M. Defoin-Platel, S. Worner, N. Kasabov, Integrated feature and parameter optimization for an evolving spiking neural network: exploring heterogeneous probabilistic models, Neural Netw. 22 (5) (2009) 623–632.
[12] J. Lazzaro, J. Wawrzynek, A multi-sender asynchronous extension to the AER protocol, in: W.J. Dally, J.W. Poulton, A.T. Ishii (Eds.), ARVLSI, IEEE Computer Society Press, Chapel Hill, NC, USA, 1995, pp. 158–169.
[13] R. Serrano-Gotarredona, M. Oster, P. Lichtsteiner, A. Linares-barranco, R. Paz-vicente, F. Gomez-rodriguez, L. Camunas-mesa, R. Berner, M. Rivas-perez, T. Delbruck, S.-c. Liu, R. Douglas, P. Hafliger, G. Jimenez-moreno, A.C. Ballcels, T. Serrano-gotarredona, A.J. Acosta-jimenez, B. Linares-barranco, CAVIAR: A 45k Neuron, 5M Synapse, 12G Connects/s AER hardware sensory-processing-learning-actuating system for high-speed visual object recognition and tracking, IEEE Trans. Neural Netw. 20 (9) (2009) 1417–1438.
[14] K. Dhoble, N. Nuntalid, G. Indiveri, N.K. Kasabov, Online spatio-temporal pattern recognition with evolving spiking neural networks utilising address event representation, rank order, and temporal spike learning, in: International Joint Conference on Neural Networks, Brisbane, Australia, 2012, pp. 1–7.
[15] N. Kasabov, V. Feigin, Z.-G. Hou, Y. Chen, L. Liang, R. Krishnamurthi, M. Othman, P. Parmar, Evolving spiking neural networks for personalised modelling, classification and prediction of spatio-temporal patterns with a case study on stroke, Neurocomputing 134 (2014) 269–279.
[16] S. Ghosh-Dastidar, H. Adeli, Improved spiking neural networks for EEG classification and epilepsy and seizure detection, Integr. Comput. Aided. Eng. 14 (3) (2007) 187–212.
[17] S.G. Wysoski, L. Benuskova, N.K. Kasabov, Evolving spiking neural networks for audiovisual information processing, Neural Netw. 23 (7) (2010) 819–835.
[18] J.A. Wall, L.J. McDaid, L.P. Maguire, T.M. McGinnity, Spiking neural network model of sound localization using the interaural intensity difference, IEEE Trans. Neural Netw. Learn. Syst. 23 (4) (2012) 574–586.
[19] T. Rumbell, S.L. Denham, T. Wennekers, A spiking self-organizing map combining STDP, oscillations, and continuous learning, IEEE Trans. Neural Netw. Learn. Syst. 25 (5) (2014) 894–907.
[20] B.J. Grzyb, E. Chinellato, G.M. Wojcik, W.A. Kaminski, Facial expression recognition based on Liquid State Machines built of alternative neuron models, in: International Joint Conference on Neural Networks, IEEE, Atlanta, GA, 2009, pp. 1011–1017.
[21] J.-H. Shin, D. Smith, W. Swiercz, K. Staley, J.T. Rickard, J. Montero, L.A. Kurgan, K.J. Cios, Recognition of partially occluded and rotated images with a network of spiking neurons, IEEE Trans. Neural Netw. 21 (11) (2010) 1697–1709.
[22] S.G. Wysoski, L. Benuskova, N. Kasabov, Fast and adaptive network of spiking neurons for multi-view visual pattern recognition, Neurocomputing 71 (2008) 2563–2575.
[23] Z. Zhang, Q. Wu, Z. Zhuo, X. Wang, L. Huang, Wavelet transform and texture recognition based on spiking neural network for visual images, Neurocomputing 151 (3) (2014) 985–995.
[24] C. Koch, I. Segev, The role of single neurons in information processing, Nat. Neurosci. 3 (2000) 1171–1177.
[25] M.-O. Gewaltig, M. Diesmann, NEST (NEural Simulation Tool), Scholarpedia 2 (4) (2007) 1430.
[26] J. Wang, A. Belatreche, L. Maguire, T.M. McGinnity, An online supervised learning method for spiking neural networks with adaptive structure, Neurocomputing 144 (2014) 526–536.
[27] J. Kominek, A.W. Black, The CMU Arctic Speech Databases, in: ISCA Speech Synthesis Work., 2004, pp. 223–224.
[28] M. Adjouadi, D. Sanchez, M. Cabrerizo, M. Ayala, P. Jayakar, I. Yaylali, A. Barreto, Interictal spike detection using the Walsh transform, IEEE Trans. Biomed. Eng. 51 (5) (2004) 868–872.
[29] M. Cabrerizo, M. Ayala, M. Goryawala, P. Jayakar, M. Adjouadi, A new parametric feature descriptor for the classification of epileptic and control EEG records in pediatric population, Int. J. Neural Syst. 22 (2) (2012) 1250001.
[30] F. Ponulak, A. Kasinski, Supervised learning in spiking neural networks with ReSuMe: sequence learning, classification, and spike shifting, Neural Comput. 22 (2) (2010) 467–510.
[31] S. Ghosh-Dastidar, H. Adeli, A new supervised learning algorithm for multiple spiking neural networks with application in epilepsy and seizure detection, Neural Netw. 22 (10) (2009) 1419–1431.
[32] J.J. Wade, L.J. Mcdaid, J.A. Santos, H.M. Sayers, SWAT: a spiking neural network training algorithm for classification problems, IEEE Trans. Neural Netw. 21 (11) (2010) 1817–1830.
[33] A. Mohemmed, S. Schliebs, S. Matsuda, N.K. Kasabov, S.P.A.N. Spike, Pattern association neuron for learning spatio-temporal spike patterns, Int. J. Neural Syst. 22 (4) (2012) 1250012.
[34] Y. Choe, R. Miikkulainen, Self-organization and segmentation in a laterally connected orientation map of spiking neurons, Neurocomputing 21 (1998) 139–157.
[35] P. Gómez-Vilda, J.M. Ferrández-Vicente, V. Rodellar-Biarge, Simulating the phonological auditory cortex from vowel representation spaces to categories, Neurocomputing 114 (2013) 63–75.
[36] T.J. Sejnowski, Time for a new neural code? Nature 376 (6) (1995) 21–22.
[37] S. Sargolzaei, M. Cabrerizo, M. Goryawala, A.S. Eddin, M. Adjouadi, Functional connectivity network based on graph analysis of scalp EEG for epileptic classification, in: Signal Processing in Medicine and Biology Symposium, Brooklyn, NY, 2013, pp. 1–4.
[38] T. Gandhi, B.K. Panigrahi, S. Anand, A comparative study of wavelet families for EEG signal classification, Neurocomputing 74 (17) (2011) 3051–3057.
[39] M. Ayala, M. Cabrerizo, P. Jayakar, M. Adjouadi, Subdural EEG classification into seizure and nonseizure files using neural networks in the gamma frequency band, J. Clin. Neurophysiol. 28 (1) (2011) 20–29.
[40] M. Tito, M. Cabrerizo, M. Ayala, P. Jayakar, M. Adjouadi, A comparative study of intracranial EEG files using nonlinear classification methods, Ann. Biomed. Eng. 38 (1) (2010) 187–199.

Zhenzhong Wang received the B.S. degree in Applied Physics from Southeast University, China, in 2006, and M.S. degree in Solid State Electronics from Southeast University. He is currently a Ph.D. student with the Department of Electrical and Computer Engineering of Florida International University. His research interest including machine learning, spiking neural networks, and bio-signal processing.

Lilin Guo received her M. Eng. degree in control theory and control engineering from Huazhong University of Science and Technology (HUST) in China, in 2009, and the B.Sc. degree in Information and Computation Science from Wuhan University of Technology (WHUT) in China, in 2006. She is currently working toward the Ph. D. degree with the Department of Electrical and Computer Engineering, Florida International University, Miami, FL. Her research interest including machine learning, spiking neural networks, signal processing, nonlinear and hybrid system.

Malek Adjouadi is a Professor with the department of Electrical and Computer Engineering at Florida International University. He is the founding director of the Center for Advanced Technology and Education funded by the National Science Foundation, since 1993. He received his B.S. degree from Oklahoma State University and his M.S. and Ph.D. degrees all in Electrical Engineering from the University of Florida. Malek's earlier work on computer vision to help persons with blindness led to his testimony to the US Senate on the committee of Veterans Affairs on the subject of technology to help persons with disabilities. His research interests are in image and signal processing with applications to neuroscience and assistive technology research.